Published in final edited form as:
Behav Brain Res. 2013 January 1; 236(1): 35–47. doi:10.1016/j.bbr.2012.08.020.

High-throughput screening of stem cell therapy for globoid cell leukodystrophy using automated neurophenotyping of twitcher mice

Brittni A. Scruggs[a], **Annie C. Bowles**[b], **Xiujuan Zhang**[a], **Julie A. Semon**[a], **Evan J. Kyzar**[c], **Leann Myers**[d], **Allan V. Kalueff**[c], and **Bruce A. Bunnell**[a,c,*]

[a]Center for Stem Cell Research and Regenerative Medicine, Tulane University School of Medicine, 1430 Tulane Avenue, SL-99, New Orleans, LA 70112, USA

[b]Department of Cell and Molecular Biology, Tulane University, 2000 Percival Stern Hall, 6400 Freret Street, New Orleans, LA 70118, USA

[c]Department of Pharmacology, Tulane University School of Medicine, 1430 Tulane Avenue, SL-83, New Orleans, LA 70112, USA

[d]Department of Biostatistics & Bioinformatics, Tulane University School of Public Health and Tropical Medicine, 1440 Canal Street, Suite 2001, New Orleans, LA 70112, USA

Abstract

Globoid cell leukodystrophy (Krabbe's disease) is an autosomal recessive neurodegenerative disorder that results from the deficiency of galactosylceramidase, a lysosomal enzyme involved in active myelination. Due to the progressive, lethal nature of this disease and the limited treatment options available, multiple laboratories are currently exploring novel therapies using the mouse model of globoid cell leukodystrophy. In order to establish a protocol for motor function assessment of the twitcher mouse, this study tested the capability of an automated system to detect phenotypic differences across mouse genotypes and/or treatment groups. The sensitivity of this system as a screening tool for the assessment of therapeutic interventions was determined by the administration of murine bone marrow-derived stem cells into twitcher mice via intraperitoneal injection. Animal behavior was analyzed using the Noldus EthoVision XT7 software. Novel biomarkers, including abnormal locomotion (e.g., velocity, moving duration, distance traveled, turn angle) and observed behaviors (e.g., rearing activity, number of defecation boli), were established for the twitcher mouse. These parameters were monitored across all mouse groups, and the automated system detected improved locomotion in the treated twitcher mice based on the correction of angular velocity, turn angle, moving duration, and exploratory behavior, such as thigmotaxis. Further supporting these findings, the treated mice showed improved lifespan, gait, wire hang ability, twitching severity and frequency, and sciatic nerve histopathology. Taken together, these data demonstrate the utility of computer-based neurophenotyping for motor

*Corresponding author: Bruce A. Bunnell, PhD, Tulane University School of Medicine, 1430 Tulane Avenue, SL-99, New Orleans, LA, USA 70112, Phone: 1-(504) 988-7711, Fax: 1-(504) 988-7710, bbunnell@tulane.edu.

Disclosure of Potential Conflicts of Interest
No potential conflicts of interest were disclosed.

function assessment of twitcher mice and support its utility for detecting the efficacy of stem cell-based therapy for neurodegenerative disorders.

Keywords

Globoid cell leukodystrophy; Noldus Technology; EthoVision XT7; behavioral phenotype; twitcher mouse; mesenchymal stem/stromal cells

1. Introduction

Globoid cell leukodystrophy (GLD; Krabbe's Disease) is an autosomal recessive neurodegenerative disorder caused by deficient galactosylceramidase (GALC), a lysosomal enzyme responsible for the metabolism of glycolipids during active myelination [1–5]. A rapidly progressive disorder, GLD affects both the central and peripheral nervous systems and presents most commonly as a lethal course causing death by the age of 2 years [2, 6]. The twitcher mouse model is an authentic model of human GLD that resulted from a spontaneous mutation of the GALC gene (*Galc*^{twi}) [7]. Studied mainly in the C57Bl/6 genetic background, the twitcher mouse presents at post natal day (PND) 14–15 with symptoms of motor function deterioration, weight reduction, and decreased activity. If left untreated, twitcher mice will experience rapid motor and neurological deterioration and death by PND40 [2, 7, 8]. Pathological features in this mouse model are similar to those in the affected human, including central and peripheral demyelination, thus highlighting the utility of these mice for studying human GLD [8–10].

Experimental treatments in the twitcher mouse have shown modest improvements in survival, although all treated animals, regardless of therapeutic approach, experience severe motor and neurological deterioration before dying prematurely [3, 11–13]. The severity and progressive nature of GLD, in addition to the lack of effective treatment options, highlight the need for further development of innovative therapeutic approaches. Therapeutic studies using the twitcher mouse must aim to correct neurological and motor abnormalities in order to achieve motor function and quality of life improvement in GLD patients. Specifically, add-on therapies that target the peripheral nervous system and/or increase GALC enzyme levels are actively being tested for development of a treatment that, combined with CNS therapy, would alleviate symptoms related to widespread demyelination [14].

In order to evaluate the efficacy of new treatment combinations, measurements of motor function become necessary for comparison across treatment groups. For this purpose, many research teams have routinely used the wire hang test to assess strength in the hind legs [13, 15–18], gait testing [15, 19], twitcher frequency and severity scoring [15, 16, 20], and the rotarod test to assess balance, coordination, and strength [13, 16–18]. However, there is no agreed screening protocol, and mouse groups cannot be accurately compared across laboratories due to differences in testing regimens (e.g., number of weekly tests, combination of tests performed) and scoring systems (e.g., wire hang scores defined by hang time vs. wire grasping difficulty). Additionally, the validity of observational testing is compromised by observational and analysis biases, especially when an observer is not blinded to the treatment group. Studies that provide only survivability and body weight data avoid such biases, yet the absence of motor function data decreases the translatability of a study while relying on expensive and time-consuming molecular studies to compare treatment groups that may have no effect on a patient's presentation. The goal of the present study was to apply computer-based video-tracking to detect quantitative differences in behavior and motor activity between wild-type and twitcher mice of various treatment groups. Automated neurophenotyping has become widely used to accurately monitor mouse

behaviors and physiological parameters for motor function assessment [21–24], and application of this technology to the twitcher mouse model may improve sensitivity and reliability of motor function assessment and provide a means of high-throughput therapeutic screening for GLD that can be reproduced consistently in various laboratories.

2. Materials and Methods

2.1. Animals

Adult (3 month old) heterozygote (Het; *Galc*$^{twi/+}$) C57Bl/6J (B6.CE-*Galc*twi/J) mice were originally obtained from The Jackson Laboratory (Bangor, ME) and used as breeder pairs to generate homozygous (Twi; *Galc*$^{twi/twi}$) twitcher mice. The established mouse colony was maintained under standard housing conditions in the pathogen-free environment of Tulane University Vivarium. Animals were housed 4–5 mice per cage with free access to food pellets and water, and the twitcher mice had access to a Diet Gel 76A nutrient fortified water gel (ClearH2O, Portland, ME) following weaning at PND 21. In total, there were six mouse groups studied: 25 untreated wild-type (WT, *Galc*$^{+/+}$), 15 BMSC treated WT (WTBMSC, *Galc*$^{+/+}$), 13 untreated heterozygote (Het, *Galc*$^{twi/+}$), 26 untreated twitcher (Twi, *Galc*$^{twi/twi}$), 19 Hank's balanced salt solution injected twitcher (HBSS, *Galc*$^{twi/twi}$), and 13 BMSC treated twitcher (BMSC, *Galc*$^{twi/twi}$) mice were used in this study. All groups were comprised of male and female mice (Tables 1 and 2). The animals were maintained on a 12:12-h light/dark cycle (lights on at 06.00 h; off at 18.00 h), and behavioral testing was consistently conducted between 14.00 and 18.00 h. All animal procedures were approved by the Institutional Animal Care and Use Committee (IACUC) at Tulane University and conformed to the requirements of the Animal Welfare Act. The specific *Galc* mutation was confirmed by real-time RT-polymerase chain reaction (PCR) on DNA obtained from anal swabs, as previously described [25].

2.2. Intraperitoneal Injections of Murine eGFPTgBMSCs

Bone marrow-derived mesenchymal stem cells (BMSCs) were obtained from male eGFP transgenic mice (C57Bl/6-Tg(UBC-GFP)30Scha/J strain; Jackson Laboratory) between 4 and 6 months of age. BMSCs were isolated and cultured from the femurs and tibias of each mouse as previously described (Ripoll & Bunnell, 2009). Passage eight murine eGFPTgBMSCs were recovered from cryopreservation in complete Iscove's modified Dulbecco's media (IMDM) media (Invitrogen, Carlsbad, CA) with 10% fetal bovine serum (Atlanta Biologicals, Lawrenceville, GA), 10% horse serum (HyClone Laboratories, Inc., South Logan, UT), 1% L-glutamine (Invitrogen), and 1% penicillin-streptomycin (Invitrogen), cultured to 70% confluency and harvested for infusion. The cells were washed thoroughly with 1X phosphate buffered saline (Invitrogen) after removing media, lifted with trypsin (Invitrogen), neutralized with an equal volume of complete media, and counted using a Countess® Automated Cell Counter (Invitrogen). The cells were centrifuged at 420*x*g for 5 minutes at room temperature. After aspiration of the media, the cell pellet was resuspended at 20,000 cells/μL with Hank's balanced salt solution (HBSS, Fisher Scientific, Pittsburgh, PA) containing calcium and magnesium but no phenol red. The cells were kept on ice for no longer than one hour prior to injection. Before injection, the cell suspension was mixed thoroughly by inversion, and a 50 μL syringe with an attached 30-gauge stainless steel needle was used to uptake he necessary volume of cells. All treated animals received injections of 10 μL of the cell suspension (2×10^5 total eGFPTgBMSCs) or HBSS into the left side of the peritoneal cavity on post natal day 5 or 6 (PND 5–6). The needle was kept immobilized for 20-s (seconds) before withdrawing to avoid leakage of the cell suspension from the injection site, and the pups were then returned to their mother.

2.3. Motor Function Testing

Beginning on PND14, motor function tests were performed three times per week to monitor the body weight, twitching frequency and severity, wire hang, and hind stride length; all data points represent the average of scores reported by two independent observers. Twitching frequency and severity were scored using the following scoring system: Frequency – no twitching (0), rare twitching and/or mild vibration (1), intermittent (i.e., twitching more often than not but with periods of no apparent twitching) (2), constant (3); Severity – complete absence (0), fine with total head control (1), mild with decreased lateral head movement (2), moderate with no head movement (3), and severe with inability to raise head (4). The hindlimb strength and control were measured by a wire hang test, where the mice were suspended by the tail and lowered onto a horizontal wire. The scale of wire hang ranged from 0 to 4, as follows: mouse could grasp the wire using its hind legs for more than 3-s (0), grasped the wire for at least 3-s with some struggling (1), grasped the wire with its hind legs for 3-s (2), fell within 3-s (3), or fell immediately (i.e., could not grasp the wire) (4). Hind stride length was measured by applying food coloring to the paws of the mice and allowing them to walk through a tube lined with graph paper as previously described [15]. The hind stride length of both the left and right back paws were measured and averaged together by an analyst who was blinded to the genotype and treatment group. Twitcher mice were euthanized once they lost 20% of their maximum body weight or became moribund. Body weight was measured three times per week beginning on PND16 and measurements were continued until the date of euthanasia.

2.4. Behavioral Analyses Using Video-tracking

Video recording of each mouse was conducted weekly using a LifeCam Cinema webcam with True 720p HD video and Debut Video Capture Software (Microsoft Corp., Redmond, WA). The webcam was positioned on a stand 40 cm above the center of a clear Plexiglas observational cylinder (13 cm in diameter, 15 cm in height). For each trial, white multipurpose paper served as the arena floor to allow for further analyses using the Ethovision XT7 software package (Noldus IT, Leesburg, VA), which detects the subjects against a monochrome background. The arena was cleaned between trials by replacement of the background paper.

Each trial began with a 3-s recording of the empty arena to establish the background image, and each mouse was then recorded for 5 min (minutes). Additionally, a highly trained and blinded observer manually recorded behavioral observations, including the latency to grooming, paw licks, body washes, defecation boli deposited, and number of digs (i.e., attempts at escaping under arena wall), as well as the number of vertical rears, including protected (wall-leaning), unprotected (paws in the air), and total (protected + unprotected) vertical rears. All video files were uploaded for analysis using the EthoVision XT7 software, and for each video, a still frame of the empty arena was used for calibration. The inner zone of the observation cylinder was defined as a circle directly in the center of the outer circle with an area equivalent to half that of the outer circle; inner and outer zones were standardized for all arenas to allow for consistent analysis of frequency and duration in each respective zone (Fig. 4c).

Data analysis was performed at 30 frames/s, and the detections of the subject's movements allowed for quantification of various spatial endpoints, such as mean velocity, total distance traveled, angular velocity, mean turn angle, inner and outer zone duration [23, 24]. After each trial, the program generated per-minute data for all specified parameters (Table 2) that could be compared across various GLD genotype and treatment groups. The program also generated JPEG images of each mouse's tracks after the 5-min recording period, and these tracks were used to visually assess and compare mouse activity in the arena. All tracks from

each treatment over the four weeks were analyzed by a blinded analyst using Image J software (U. S. National Institutes of Health, Bethesda, Maryland, http://imagej.nih.gov/ij/) [26]. The densities of the tracks were quantified in pixels using this software, and representative images were chosen based on the median value of pixels. In Figure 4, the track images of the four mouse groups taken over four weeks represent 16 different mice.

2.5. Tissue Processing and Histological Staining

Animals were euthanized by exposure to CO_2 and perfused with sterile PBS. Sciatic nerves were removed and stored at room temperature in 10% neutral buffered formalin. Paraffin-embedded sections were cut at 5 microns and mounted on Superfrost glass slides and subsequently stained with hematoxylin and eosin (HE), luxol fast blue (LFB), or periodic acid-Schiff (PAS). Slides were scanned using an Aperio ScanScope® CS instrument (Aperio Technologies, Inc., Vista, CA) at 10× and 40×. Slides were analyzed with the Aperio ImageScope viewing software using the Positive Pixel Count v9 analysis tool; specifically, the hematoxylin and eosin (HE), periodic acid-Schiff (PAS), and luxol fast blue (LFB) stains were used for identification of infiltrating immune cells, the presence of globoid cells, and myelin levels, respectively. All scanned images were used for comparison purposes, and a blinded analyst chose representative images for the LFB (WT (n=3), BMSC (n=4), and twitcher (n=7)), HE (WT (n=5), BMSC (n=4), and twitcher (n=8)), and PAS (WT (n=3), BMSC (n=4), and twitcher (n=7)) stains.

2.6. Statistical Analysis

For comparisons of body weight, wire hang, and hind stride length (Fig. 1a, e, and f), mixed models regression methods were implemented via PROC MIXED in SAS (version 9.2). For tests with a significant ($p<0.05$) time X group interaction, pairwise comparisons of least square means were made to further investigate the interaction. First, the initial time point (e.g., PND16) was compared to the last tested time point (e.g., PND40) for each mouse group. Second, the three mouse groups (WT-BMSC, BMSC, and Twi) were compared to each other at each time point for a total of 36 or 39 t-tests. To correct for multiple comparisons, the p-values were adjusted using a Bonferroni correction. Significance was determined if $p<0.0014$ for the weight and hind stride studies (36 tests) and $p<0.0012$ for the wire hang study (39 tests). All values were plotted as mean ± SEM.

Statistical analysis on the Kaplan-Meier survival curve was performed using the log rank test (Fig. 1b), and the median lifespan values were compared using a non-parametric Mann–Whitney U-test. Twitching frequency and severity were assessed only in the two twitcher mouse groups (BMSC and Twi), and exact chi-square tests were performed at each time point to test for differences between the two treatment groups (Fig. 1c and d). A total of 13 tests were performed, and thus the Bonferroni-corrected criterion for rejection of the null hypothesis was $p<0.0038$. Medians, and not means, were plotted for the twitching studies.

For the behavioral, neurophenotyping, and histological studies (Figs. 2–6), statistical analysis of three or more groups was performed using one-way analysis of variance (ANOVA) followed by pairwise comparisons of the mouse groups using Bonferroni *post-hoc* testing. Significance for the overall group effect and individual pairwise comparisons was defined as $p<0.05$. For any study where the mouse groups were monitored for three consecutive weeks (Fig. 2f) or over several minutes during a single recording (Fig. 3e), two-way ANOVA (factors: time and mouse group) with repeated measures and subsequent Bonferroni *post-hoc* testing was performed. One and two-way ANOVA tests were performed using GraphPad Prism version 4.0b for Macintosh (San Diego, CA, USA), and all values were reported as mean ± SEM.

3. Results

3.1. Weight and Longevity

Body weight was monitored three times a week for the untreated WT, BMSC-treated twitcher (BMSC), and untreated twitcher (Twi) mouse groups starting at PND16 (Fig. 1a). There were no significant differences found between males and females when comparing weights or motor function curves (data not shown); therefore, all mouse groups included both male and female mice. There was a significant interaction between mouse group and post natal day (PND) ($p<0.0001$). For the WT and BMSC groups, there was a significant weight difference between the first and last time points ($p<0.0001$), but no significant difference was found for the Twi group ($p = 0.14$). Post-hoc comparisons revealed no significant differences between the two twitcher mouse groups for any time point. The vivarial staff monitored all twitcher mice by inspection (i.e., without touching mouse cages) each morning to assess food accessibility and moribund status of all mice, and the twitcher mice were euthanized when they met the euthanasia criteria described earlier. Longevity was used as an objective measurement of therapeutic efficacy (Fig. 1b); a log rank test performed on the Kaplan-Meier survival curves showed a significant ($c^2=12.8$, $p<0.0005$) difference between the curves of the untreated and BMSC-treated groups. The median lifespan of the untreated twitcher group (36.0 days) was significantly shorter compared to the BMSC-treated mice (42.0 days; $p<0.0001$).

3.2. Behavioral Assessments Using Conventional Motor Function Tests

Twitching frequency and severity were assessed using the conventional twitching clinical scoring systems (Fig. 1c–d). There were significant differences between the treated and untreated twitcher groups at PND 18, 20, 24, 26, and 38 for twitching frequency and at PND 20, 34, 36, 38, and 40 for twitching severity ($p<0.0038$). Hind leg strength and severity of disease progression were assessed using the wire hang test (Fig. 1e), and the interaction of time and mouse group was significant ($p<0.0001$). The WT mice were capable of hanging for >3-s without struggle for all time points; however, both twitcher groups became more different from the normal mice as time passed and ultimately from each other at PND 36 and 38 ($p<0.0001$). The wire hang test was a sensitive measure of disease progression, indicated by the increase in wire hang scores over time and the finding that all untreated twitcher mice were unable to hang for 3-s (i.e., score of 3 or 4) at the time of their euthanasia. When hind stride lengths were compared (Fig. 1f), the interaction of time and mouse group was significant ($p<0.0001$), and the mice receiving the BMSC treatment had improved hind stride compared to the untreated twitchers at PND28 ($p=0.001$) and PND34–36 ($p<0.0001$).

3.3. Phenotyping of the Twitcher Mouse Using Video-tracking

Video-tracking of individual mice was performed in this study to establish endpoints sensitive to differences between the three untreated mouse groups (Table 1). For this, all untreated WT, untreated Het, and untreated Twi mice were recorded once during the PND16–22 time period, at which time the twitching symptoms of the twitcher group were mild and the motor function was not significantly affected (Fig. 1). The average ages of the WT, Het, and Twi mice recorded for this experiment were PND20.4±0.4, 21.5±0.4 and 18.3±0.6 days, respectively.

During video-tracking experiments, each mouse was placed in an observational cylinder for video-recording and manual observations for 5 min. There was a significant main effect for genotype on number of protected rears ($F(2,37)=7.9$, $p<0.001$), number of unprotected vertical rears ($F(2, 37)=7.1$, $p<0.005$), and total number of rears ($F(2,37)=11.4$, $p<0.001$). Post-hoc comparisons of the groups showed that Het ($p<0.01$) and twitcher ($p<0.001$) groups had significantly fewer total rears than the WT mice (Fig. 2a). Other manually

observed behaviors monitored for phenotypic differences between GLD genotypes were the latency to groom ($F(2, 37)=3.0$, $p=0.06$), paw lick duration ($F(2, 37)=2.5$, $p=0.10$), body/leg wash duration ($F(2, 37)=2.4$, $p=0.12$), and defecation boli ($F(2, 37)=0.1$, $p=0.87$) during the 5-min trial (Table 1).

Ethovision XT7 was utilized to analyze the videos of all three genotypes comparing different parameters to detect phenotypic differences in motor function at PND16–22. Multiple endpoints showed significant differences between the genotype groups during this time period, including moving duration (Fig. 2b, $F(2,41)=5.6$, $p<0.007$), moving frequency ($F(2,41)=3.4$, $p=0.04$), maximum velocity (Fig. 2c; $F(2,41)=8.3$, $p<0.001$), inner zone frequency (Fig. 2d, $F(2,41)=4.5$, $p<0.02$), duration of immobile bouts ($F(2,41)=5.6$, $p=0.007$) and total distance traveled (Fig. 2e; $F(2,41)=3.5$, $p<0.04$). Post-hoc comparisons revealed that spatial locomotion of the twitcher mice, assessed as any movement of the body center in excess of a defined threshold, was significantly ($p<0.01$) lower than in the WT mice (Fig. 2b). Even though the Het group appeared to have similar activity as the WT group, the maximum velocity of the Het group was significantly lower vs. the WT (Fig. 2b–d; $p<0.05$). Other parameters were analyzed at PND16–22, including mean velocity ($F(2,41)=2.8$, $p<0.08$), inner zone duration time ($F(2,41)=1.3$, $p<0.30$), total meandering ($F(2,41)=1.7$, $p<0.20$), and mean time spent immobile ($F(2,41)=0.7$, $p<0.52$) (Table 1). For several parameters, including angular velocity ($F(2,41)=1.0$, $p<0.4$) and mean turn angle ($F(2,41)=1.0$, $p<0.4$), genotype had no overt effects during PND16–22; however, over the course of this study the mice developed neurocognitive and motor deficits and significant differences between the groups became apparent in these parameters. Comparing angular velocity over three weeks for all three genotype groups, there was a significant group X time interaction ($F(4,110)=5.920$, $p<0.0001$) with the twitcher mice displaying significant deviation of angular velocity compared to WT mice at the PND23–29 and PND30–35 time points only (Fig. 2f; $p<0.001$).

3.4. Assessment of Treatment Efficiency Using Video-tracking

To further test the sensitivity of video detection of GLD mouse phenotypes, the BMSC-treated WT (WT-BMSC), BMSC-treated twitcher (BMSC), HBSS-treated twitcher (HBSS), and untreated twitcher (Twi) mice were video-recorded once during PND23–29, a period when the conventional motor function tests detected only slight, if any, differences between the BMSC-treated and untreated groups. The Twi mice were the same as those in the previously described study testing the three genotypes; thus, all mouse groups for this study were recorded once during 16–22 (data not shown) to account for this additional recording of the Twi group. Ethovision XT7 software was again used to analyze the spatial and inter-zonal locomotion for 5 min. All behavioral and spatial endpoints tested at PND16–22 for genotype effects (Table 1) were used for comparisons of all mouse groups at PND23–29 (Table 2). The average ages of the WT-BMSC, BMSC, HBSS, and Twi mice in this experiment were PND 25.2±0.4, 25.6±0.5 26.5±0.1, and 26.4±0.5, respectively. At this time point, all twitcher mice, regardless of treatment, had body weights that were significantly ($p<0.001$) lower than the WT-BMSC weights; however, by visual inspection, kyphosis of the spine, muscle wasting, and hind limb paralysis were not evident.

A one-way ANOVA with Bonferroni post-hoc testing was performed for each of the spatial and interzonal parameters for comparison between groups. Mouse group had a significant effect on average velocity ($F(3, 62)=11.1$, $p<0.0001$), maximum velocity ($F(3, 62)=5.4$, $p<0.01$), total distance traveled ($F(3, 62)=11.2$, $p<0.0001$), duration of movement bouts ($F(3, 62)=7.8$, $p<0.0005$), average moving time ($F(3, 62)=17.1$, $p<0.0001$), frequency of entering the center ($F(3, 62)=9.6$, $p<0.0005$), time spent in center ($F(3, 62)=5.1$, $p<0.01$), angular velocity ($F(3, 62)=17.6$, $p<0.0001$), average turn angle ($F(3, 62)=11.3$, $p<0.0001$) and time spent immobile ($F(3, 62)=16.6$, $p<0.0001$) (Table 2; Fig. 3–4). Further

investigation of the group differences showed that the HBSS and Twi mice both significantly differed from WT-BMSC mice in all spatial endpoints, whereas the BMSC-treated mice did not differ significantly when compared to the WT-BMSC mice (Table 2). Treated twitcher mice showed significant improvement compared to the HBSS and Twi groups in average velocity, maximum velocity, total distance traveled, frequency in center, angular velocity, average turn angle and time spent immobile ($p<0.05$; Fig. 3–4). These data suggest that the stem cell treatment, although given peripherally and at a suboptimal dose, corrected many of the abnormal neurophenotypes of the twitcher mouse during this time period. For each mouse, the total distance traveled was calculated for every 1-min time bin. Comparison of this parameter over the 5-min testing period showed that the WT-BMSC mice decreased their exploratory behavior over time, while untreated twitcher mice displayed an increase in distance traveled after min 1 (Fig. 3e). Additionally, the distance traveled by the Twi mice was lower ($p<0.05$) vs. WT-BMSC mice during min 2 and 3, whereas the BMSC-treated and HBSS-treated mice showed no significant difference compared to the WT-BMSC or Twi mouse groups for any minute of the trial (Fig. 3e).

In addition to providing quantitative measurements related to rodent locomotion, the video-tracking approach allowed track visualization from the continuous detection of the mice over the 5-min recording period. In this experiment, the tracks were arranged in the order of increasing track density for each PND age range; representative tracks were chosen for each age group as previously described. Fig. 4 shows the tracks across the four mouse groups for PND16–22, 23–29, 30–35 and 36–45. There were no overt differences between the WT-BMSC group and BMSC groups until PND30–35 when slight differences in the track density, especially in the inner zone, became apparent. The HBSS and Twi mouse tracks had strikingly lower track densities compared to the BMSC-treated group and WTBMSC mice starting at PND23–29 (Fig. 4a). Based on the track visualizations and the decreased time in the inner zone, it was evident that the non-cell treated twitcher mice exhibited higher thigmotaxis than the BMSC-treated twitcher mice (Fig. 4a–b).

Additionally, it was found that for all groups tested at PND23–29 there was no significant difference in any parameter when comparing males and females of the same mouse group (data not shown). Furthermore, for any given parameter studied, post-hoc comparisons between the HBSS-injected and untreated Twi mice showed no significant difference, suggesting that IP injections given at PND 5 or 6 do not affect any spatial or behavioral characteristics of the twitcher mouse (Table 2). Collectively, these studies demonstrated that this video-tracking approach was a sensitive tool for objectively detecting the motor function of the twitcher mouse model of GLD.

3.5. Grooming and Other Behaviors

Self-grooming is an important aspect of mouse behavior. To detect any changes in grooming activity due to the twitcher phenotype, all groups were observed for various behaviors (e.g., latency to grooming activity, paw lick duration, body/leg wash duration, number of rears, number of defecation boli, and number of digs) at PND23–29 during the 5-min trial, as described previously (Kalueff *et al.*, 2007a). Mouse group had a significant effect on number of defecations (Fig. 5e, $F(3, 46)=10.1$, $p<0.0001$), total rears (($F(3, 46)=22.6$, $p<0.0001$), as well as unprotected ($F(3, 46)=23.2$, $p<0.0001$) and protected rears ($F(3, 46)=11.5$, $p<0.0001$). Post-hoc testing showed that the untreated twitcher mice had significantly lower rearing activity (all rearing types, $p<0.0001$) compared to the WT-BMSC group (Fig. 5a–c; Table 2). This study provided evidence that the BMSC treatment also significantly differed from WT-BMSC mice in total ($p<0.01$) and unprotected rears ($p<0.001$) (Fig. 5a–b), and no improvement due to cell treatment was seen at this time point in the twitcher mice. There was also a significant main effect on digging activity ($F(3, 46)=35.38$, $p<0.0001$), where the BMSC-treated mice had increased number of escape attempts (i.e., digs) compared to all

other mouse groups ($p<0.001$) (Fig. 5d). Other manually observed behaviors at this time period that did not show significant group effects were latency time to first grooming bout (Fig. 5f, $F(3, 46)=0.71$, $p<0.55$), total duration spent paw licking ($F(3, 46)=0.62$, $p<0.57$), and total duration spent body washing ($F(3, 46)=0.62$, $p<0.57$).

3.6. Histological Analysis

Hematoxylin and eosin (HE), luxol fast blue (LFB), and periodic acid-Schiff (PAS) staining performed on the sciatic nerves of WT-BMSC, BMSC-treated twitcher, and untreated twitcher mice showed a decrease in the number of apoptotic cells in the PNS after IP administration of BMSCs (Fig. 6a, 40X, white arrows). In fact, no cells resembling apoptotic cells or necrotic debris were found in any sciatic nerves obtained from WT-BMSC or BMSC-treated twitcher mice. The PAS stain showed more enlarged cells, likely macrophages, when comparing the untreated twitcher to the BMSC-treated sciatic nerves (Fig. 6a, black arrows). Based on the percentage of calculated strong pixels, corresponding to the dark nuclei and cytoplasm of infiltrating immune cells, there was a significant increase in the number of infiltrating cells in both the treated and untreated twitcher groups (Fig. 6b). There was a significant decrease in the number of weak pixels in the LFB stain when comparing the untreated twitcher sciatic nerves to those of the WT-BMSC mice. However, post-hoc comparisons between the two treatment groups indicated that the BMSC treatment significantly increased the LFB staining intensity in the nerves at the time of euthanasia (Fig. 6c). The histopathological data supported findings of the motor function tests and computer-automated system by also detecting improvements in the twitcher mouse after peripheral administration of BMSCs.

4. Discussion

4.1. Detection of phenotypic differences in GLD mice using automated video-tracking

In order to establish the most sensitive endpoints using video-tracking, groups of untreated WT, Het, and Twi mice were recorded at PND16–22, a period when these mice are indistinguishable by weight, hind stride length, and wire hang ability (Fig. 1). The data (Fig. 2b–e) indicate that video-tracking can indeed objectively detect differences between the WT, Het and Twi mice even when the differences are not yet evident to the investigator using traditional phenotyping approaches. For example, several ‘automated’ endpoints (e.g., maximum velocity, duration of time spent in motion, total distance traveled, moving frequency, and number of times entering inner zone) were sensitive to GLD genotype. Unexpectedly, the mutant mice move more slowly yet perform sharper turns at a higher angular velocity; this abnormal turning behavior in mice may represent altered spatial patterning [27], which, in conjunction with hypolocomotion, can be due to reduced myelin turnover at a time when myelin production is rapidly increasing [7]. These novel findings of neurobehavioral phenotypic differences between the genotypes are consistent with the slower reaction times, altered spatial cognition, and motor and cognitive impairment in affected GLD patients and carriers with <25% of normal GALC activity levels [28].

Observational studies of twitcher and WT mice by Olmstead showed no significant genotype differences at PND15–20 when comparing neurological development and observed motor activity of untreated mice [18]. Similarly, the traditional (observational) motor function tests of this study were unable to detect significant differences during this time period. Our study showed that computer-automated analysis of mouse locomotion provides multiple quantitative measurements of parameters that cannot be accurately assessed through manual observation. Since computer-automated mouse tracking improves inter-analyzer consistency of scoring and allows for quick processing of large amounts of

data [29], such approaches can be used to reliably compare multiple cohorts without introducing observational and analysis biases.

4.2. Automated mouse tracking as a tool for evaluating therapeutic benefit in treated GLD mice

Since data generated using EthoVision XT7 clearly distinguished WT, Het and Twi mouse phenotypes based on changes in their behavioral parameters, it was hypothesized that this approach may also be sensitive to treatment effects, specifically the therapeutic effectiveness of BMSCs administered peripherally in the twitcher mice. We administered a total number of cells that, based on previous studies of mouse IP injections [30, 31], are considered extremely low. Nevertheless, automated video-tracking proved capable of detecting differences between the BMSC-treated and HBSS-injected or untreated Twi mice during the PND23–29 time period. In contrast, the common rotarod test is unable to distinguish between twitcher mice of different treatment groups until PND27–32 [16]. Comparisons of spatial and inter-zonal parameters showed that the untreated Twi mice significantly differed from WT-BMSC mice in all endpoints; however, the BMSC-treated mice were similar to the WT-BMSC cohort and were found to have corrected neurophenotypes compared to the HBSS or Twi groups for angular velocity, mean turn angle, time spent immobile, and number of times entering the inner zone. The alteration of these parameters solely in the non-cell treated twitcher groups suggests that the BMSC treatment increased motor activity and corrected spatial impairment (Fig. 3).

Additionally, for each mouse group, analysis of the total distance traveled over time showed that the WT-BMSC mice reduced their exploratory behavior over time, while the untreated twitcher mice displayed an increase in distance traveled after minute 1. These data suggest that untreated twitcher mice may have cognitive impairments inhibiting their ability to recognize environments as no longer being novel; HBSS-injected mice showed a constant distance traveled across all minutes. Based on the track visualizations and less time spent in the inner zone, the untreated and HBSS-injected twitcher mice exhibited thigmotaxis more than the BMSC-treated twitcher mice. Peripheral locomotion has been widely used as a measure of anxiety-related behavior [32, 33], and other groups have reported thigmotaxis during an open field test of twitcher mice [18]. Based on thigmotaxis improvement, it is possible that the BMSC treatment decreases anxiety; however, future studies to test this possibility will include assessment of thigmotaxis and exploratory behavior in the twitcher mouse after administration of pain relieving and/or anxiolytic drugs using a larger arena area.

Overall, the beneficial effects of the BMSC treatment were clearly demonstrated in this study using the automated video-tracking approach, and are supported by the extended lifespan and improved histopathology of the treated mice compared to the untreated twitcher group. Furthermore, this high-throughput therapeutic screening approach allows an investigator to reliably assess whether a treatment improves the clinical presentation of the twitcher mouse, thereby optimizing the selection of treatment that is most beneficial for the affected animals. Although automated systems are currently being implemented as screening tools for other animal models, it is imperative to demonstrate the utility of such a system for any newly tested model in addition to defining biomarkers (i.e., certain behaviors or parameters) that are specific to the animal's phenotype. The behavioral biomarkers discussed herein are novel and indicate a promising future for automated systems in studying the Twi mouse. In performing this study, our lab has already been able to utilize this screening method for Twi mice receiving IP injections of BMSCs at higher dosages and intracerebroventricular (ICV) injections, and preliminary results indicate a complete correction of spatial parameters for longer periods of time with significant differences between the BMSC-treated and untreated twitcher mice (data not shown). It is therefore

likely that this system can be used over time for all treatment groups as a means to measure disease progression and also as a quantitative method for comparing treatment groups.

4.3. Effects of GLD on mouse grooming and rearing behaviors

Rodent grooming and homecage activity are highly sensitive to various experimental manipulations (e.g., toxins, stress, or genetic mutations), and the frequency and duration of such behaviors can be monitored to characterize such effects [34, 35]. Early works have implicated grooming as a behavioral biomarker in GLD [18], and given the growing recognition of the importance of grooming in mouse behavioral responses and the relation to complex motor behaviors [21, 34, 36, 37], grooming is an appropriate motor phenotype to assess in these mice. A detailed behavioral analysis of the twitcher mouse was performed by Olmstead, and his findings showed altered grooming (e.g., increased paw licking and face washing) and decreased rearing when compared to WT mice [18]. Consistent with these findings, the present study also showed that the twitcher mice differed behaviorally from the WT-BMSC mice in grooming (e.g., increased paw licking) and rearing behavior. The most striking difference was their ability to perform vertical rearing during PND16–22 and 23–29. Although protected rearing and unprotected rearing are similarly affected at PND16–22 (Table 1), the protected rears are performed more frequently than unprotected rears in all twitcher groups at PND 23–29 (Table 2). Unprotected rearing must be performed without a wall and requires pure hind limb strength, therefore as GLD progresses and motor function declines the twitcher mice exhibit less vertical movements compared to protected rearing. These data suggest that the affected mice, after developing significant hind leg weakness, are unable to support the vertical movement and twisting body positions necessary to complete such exploratory behavior. This is in agreement with other mutant mouse models (e.g., weaver mice) that are also unable to complete grooming or exploratory behaviors that require stable postures [38]. Interestingly, the BMSC-treated group was able to perform more protected and total rears than the untreated mice at PND23–29, although no significance was found in post-hoc comparisons. For both this study and the Olmstead study, no rearing activity could be documented for any twitcher mouse after PND30 [18]. The BMSC mice were also capable of digging, an activity never displayed in any other mouse group; such a finding should be further investigated to determine if this treatment results in abnormal hyperactivity of the mice.

The current study suggests that manual observations of rearing behavior, movement bouts, and overall grooming behavior provide a relevant means to assess disease progression and quality of life for twitcher mice and, when combined with quantitative data generated from video-tracking, can serve as a sensitive measure of genotypic differences and treatment effectiveness for GLD mice. Improvement in protected rearing, thigmotaxis, and locomotor activity suggest that a single, low dose peripheral injection of BMSCs increases hind leg strength and improves motor coordination of the twitcher mouse. This finding is consistent with recent knowledge that mouse BMSCs home to areas of neurological damage to provide robust neuroprotective and anti-inflammatory effects [15, 39].

4.4. Intraperitoneal administration of BMSCs as therapy for the twitcher mouse model of GLD

Stem cell-based therapy has shown tremendous promise in preclinical trials of many different lysosomal storage diseases, and the mechanisms of repair and therapeutic benefits are extensive. BMSCs are capable of self-renewal and differentiation into a wide range of cell types (e.g., osteocytes, adipocytes, chondrocytes, etc.), thus making them a promising therapeutic candidate for restoration of damaged tissue [40, 41]. In addition to being accessible for harvesting in clinical settings and easily expanded in culture, BMSCs are known to express GALC, modulate immune reactions *in vitro*, and do not elicit an

immunological response *in vivo* [40, 42–44]. In light of these findings, IP injections of stem cells were administered to twitcher mouse pups in order to target the inflammation in the peripheral nervous system. The data reported here indicate that BMSCs, administered at a suboptimal dose, can modestly improve the motor activity and lifespan of the twitcher mouse when administered peripherally. Twitcher peripheral nerves exhibit myelin sheath degeneration, axonal death, and infiltration of macrophages (i.e., globoid cells) with PAS-positive cytoplasm [45–47]. In the present study, histological staining of BMSC-treated WT, BMSC-treated twitcher and untreated twitcher mouse sciatic nerves clearly provide evidence that a single IP injection of BMSCs increases LFB staining intensity and decreases the number of apoptotic cells and possible globoid cells in the PNS. The increased number of cell nuclei in the untreated Twi group could be a result of infiltrating immune cells or increased Schwann cell proliferation [46, 47]. Notably, however, the treated sciatic nerves were not void of infiltrating cells or myelin destruction, suggesting that the low number of injected BMSCs was not sufficient to treat this pathogenic aspect.

4.5. Clinical relevance of motor function improvement in the twitcher mouse

With multiple types (e.g., early infantile, late infantile, juvenile, adult) of GLD and over 75 known mutations, the clinical presentation of the affected human patient is highly variable [48, 49]. However, all patients diagnosed with GLD develop motor symptoms [48]. Specifically, the early-onset form of GLD (3–6 months) commonly presents with increased muscular tonus, early coordination disturbance, limb stiffness, poor head control, hyperextension and spasticity, and slowed motor nerve conduction velocity [48, 50–52]. The majority of late-infantile GLD patients (7–36 months) initially presents with gait abnormalities, such as clumsiness, inability to maintain sitting or standing positions, and increased muscle tone, before progressing to cerebellar ataxia and possible spastic quadriplegia [49, 50, 53]. The development and worsening of these symptoms are highly monitored in these patients, especially because the early stages of GLD can appear normal using computed tomography and magnetic resonance imaging [49, 51]. Although the twitcher mouse model differs from the human patient in many aspects (e.g., lifespan), the presentation of motor symptoms in the twitcher mouse is similarly progressive and debilitating.

GLD has been divided into three distinct symptomatic stages; Stage 1 of human GLD is characterized by limb stiffness, Stage 2 by severe motor deterioration, and Stage 3 by no spontaneous movement [54]. The authors hypothesize that these stages correlate to the three time periods explored in this study. During the PND16–22 time period, the twitcher mouse has decreased total distance traveled, velocity, time spent in motion, and rearing activity (Table 1), which are symptoms likely related to limb stiffness, decreased motor nerve velocity, and weakness of the hind legs. Motor symptoms progress rapidly in the mouse, and all spatial parameters tested during the later PND23–29 time point are significantly affected in the twitcher mouse (Table 2). Specific symptoms, such as abnormal turning behavior, can be directly related to GLD patients, who can present with a slow, rigid, and ataxic gait, particularly during turns, that is not proportional to any effect of visual impairment [49, 50, 53, 55]. Although defecation scores are usually high in anxious mice [36], the twitcher mice produce less boli than WT-BMSC mice, likely due to their reduced appetite and decreased food consumption. Similarly, the GLD patient often has feeding difficulties, problems with swallowing, and a reduced appetite [48, 49, 52, 53]. Like many end-stage GLD patients, the twitcher mouse eventually exhibits paralysis and extreme emaciation [9, 10].

Although posturing and the specifics of motor symptoms differ between human and mouse GLD, it is clear that both GLD forms are severely affected in motor function. The mouse presents with a generalized sensorimotor demyelinating polyneuropathy, which is similar to human GLD in pathophysiology and presentation [49]; therefore, it is likely that

improvement in spatial parameters in the mouse model will directly correlate to improvements in the human patient. Gait difficulties, which are present in over 80% of lateinfantile GLD patients [49], would likely be minimized, if not corrected, if stem cell-based therapy were optimized to correct such abnormalities in the twitcher mouse.

5. Conclusion

This study aimed to evaluate the effectiveness of automated analysis of video-recorded mouse behavior in an open-field type paradigm. Collectively, the data strongly support the utility of computer-based neurophenotyping for in-depth assessment of motor phenotype in a mouse model for GLD combined with assessment of treatment effects. Our findings support application of automated procedures for increasing sensitivity and efficacy of behavioral phenotyping. This study also identified several novel biomarkers of the twitcher mouse that will serve as markers of disease progression and will help establish novel addon therapies targeting specific behavioral abnormalities (e.g., thigmotaxis). Thus, the sophisticated phenotyping tools utilized in this study could be of benefit in providing an efficient, unbiased method of assessment that also enhances the biological interpretation of treatment when performed with molecular studies.

The administration of a suboptimal dose of mouse BMSCs through IP injection improved the phenotype of the twitcher mouse as determined by motor function testing, automated neurophenotyping, modest improvement in lifespan, and improved peripheral nerve histopathology. Achieving such improvements with a non-invasive administration method indicates a promising future for stem cells as a novel therapeutic for patients affected with globoid cell leukodystrophy or other glycosphingolipid storage diseases. We are planning to combine video-tracking methods and manual observations with histological and enzymatic data to assess the true effects of BMSCs on both the molecular level and the quality of life of these affected mice in order to optimize the dose, timing, and route of administration for stem cell treatment in the twitcher mouse model.

Acknowledgments

The authors thank Siddharth Gaikwad, Jeremy Green and the Neurophenotyping Core at Tulane University School of Medicine for their instruction, advice, and suggestions regarding the video recording studies, and the veterinary and vivarial staff of the TUHSC Animal Facility for the daily care of the mice. The authors also thank Shijia Zhang for help in the preparation of the mouse BMSCs, Katie Imhof for assistance with the motor function tests, Dr. Ryan Bonvillain for assistance in analyzing the histological samples, and Dina Gaupp and Claire Llamas in the Tulane Histology Core for performance of the histological staining for this study. The research was supported by grant number R21-NS059665 National Institutes of Neurological Disorders and Stroke, National Institutes of Health and Tulane University.

Abbreviations

GLD	globoid cell leukodystrophy
MSC	mesenchymal stromal cell
GALC	galactosylceramidase
BMT	bone marrow transplant
BMSC	bone marrow-derived multipotent stromal cell
GVHD	graft vs host disease
CNS	central nervous system
PNS	peripheral nervous system

iNOS	inducible nitric oxide synthase
GFP	green fluorescent protein
eGFPTgBMSC	enhanced green fluorescent protein transgenic BMSC
AAALAC	Association for Assessment and Accreditation of Laboratory Animal Care
IACUC	Institutional Animal Care and Usage Committee
PND	postnatal day
HBSS	Hank's Buffered Salt Solution
IMDM	Iscove's modified Dulbecco's media
ANOVA	analysis of variance
Twi	twitcher mouse
WT	normal wild-type mouse
Het	heterozygote mouse
HE	Hematoxylin and Eosin
LFB	Luxol Fast Blue
PAS	Periodic Acid-Schiff
IP	intraperitoneal

References

1. Suzuki K, Suzuki Y. Globoid cell leucodystrophy (Krabbe's disease): deficiency of galactocerebroside beta-galactosidase. Proc Natl Acad Sci U S A. 1970 Jun; 66(2):302–309. [PubMed: 5271165]
2. Kolodny, EH. Globoid Leukodystrophy. Elsevier Science; 1996.
3. Rafi MA, Zhi Rao H, Passini MA, Curtis M, Vanier MT, Zaka M, et al. AAV-mediated expression of galactocerebrosidase in brain results in attenuated symptoms and extended life span in murine models of globoid cell leukodystrophy. Mol Ther. 2005 May; 11(5):734–744. [PubMed: 15851012]
4. Sakai N. Pathogenesis of leukodystrophy for Krabbe disease: molecular mechanism and clinical treatment. Brain Dev. 2009 Aug; 31(7):485–487. [PubMed: 19332366]
5. Svennerholm L, Vanier MT, Mansson JE. Krabbe disease: a galactosylsphingosine (psychosine) lipidosis. Journal of lipid research. 1980 Jan; 21(1):53–64. [PubMed: 7354254]
6. De Gasperi R, Gama Sosa MA, Sartorato EL, Battistini S, MacFarlane H, Gusella JF, et al. Molecular heterogeneity of late-onset forms of globoid-cell leukodystrophy. Am J Hum Genet. 1996 Dec; 59(6):1233–1242. [PubMed: 8940268]
7. Suzuki K, Taniike M. Murine model of genetic demyelinating disease: the twitcher mouse. Microsc Res Tech. 1995 Oct 15; 32(3):204–214. [PubMed: 8527855]
8. Suzuki K, Suzuki K. The twitcher mouse: a model for Krabbe disease and for experimental therapies. Brain pathology (Zurich, Switzerland). 1995 Jul; 5(3):249–258.
9. Kobayashi T, Yamanaka T, Jacobs JM, Teixeira F, Suzuki K. The Twitcher mouse: an enzymatically authentic model of human globoid cell leukodystrophy (Krabbe disease). Brain Res. 1980 Dec 8; 202(2):479–483. [PubMed: 7437911]
10. Wenger DA. Murine, canine and non-human primate models of Krabbe disease. Mol Med Today. 2000 Nov; 6(11):449–451. [PubMed: 11074371]
11. Biswas S, Biesiada H, Williams TD, LeVine SM. Delayed clinical and pathological signs in twitcher (globoid cell leukodystrophy) mice on a C57BL/6 x CAST/Ei background. Neurobiology of disease. 2002 Aug; 10(3):344–357. [PubMed: 12270695]

12. LeVine SM, Pedchenko TV, Bronshteyn IG, Pinson DM. L-cycloserine slows the clinical and pathological course in mice with globoid cell leukodystrophy (twitcher mice). Journal of neuroscience research. 2000 Apr 15; 60(2):231–236. [PubMed: 10740228]

13. Lin D, Donsante A, Macauley S, Levy B, Vogler C, Sands MS. Central nervous system-directed AAV2/5-mediated gene therapy synergizes with bone marrow transplantation in the murine model of globoid-cell leukodystrophy. Mol Ther. 2007 Jan; 15(1):44–52. [PubMed: 17164774]

14. Miranda CO, Teixeira CA, Liz MA, Sousa VF, Franquinho F, Forte G, et al. Systemic Delivery of Bone Marrow-Derived Mesenchymal Stromal Cells Diminishes Neuropathology in a Mouse Model of Krabbe's Disease. Stem Cells. 2011 Nov; 29(11):1738–1751. [PubMed: 21898691]

15. Ripoll CB, Flaat M, Klopf-Eiermann J, Fisher-Perkins JM, Trygg CB, Scruggs BA, et al. Mesenchymal-Lineage Stem Cells Have Pronounced Anti-Inflammatory Effects in the Twitcher Mouse Model of Krabbe's Disease. Stem Cells. 2010 Nov 9.

16. Wicks SE, Londot H, Zhang B, Dowden J, Klopf-Eiermann J, Fisher-Perkins JM, et al. Effect of intrastriatal mesenchymal stromal cell injection on progression of a murine model of Krabbe disease. Behav Brain Res. 2011 Dec; 225(2):415–425. [PubMed: 21840342]

17. Lin D, Fantz CR, Levy B, Rafi MA, Vogler C, Wenger DA, et al. AAV2/5 vector expressing galactocerebrosidase ameliorates CNS disease in the murine model of globoidcell leukodystrophy more efficiently than AAV2. Mol Ther. 2005 Sep; 12(3):422–430. [PubMed: 15996520]

18. Olmstead CE. Neurological and neurobehavioral development of the mutant 'twitcher' mouse. Behav Brain Res. 1987 Aug; 25(2):143–153. [PubMed: 3675825]

19. Lee WC, Courtenay A, Troendle FJ, Stallings-Mann ML, Dickey CA, DeLucia MW, et al. Enzyme replacement therapy results in substantial improvements in early clinical phenotype in a mouse model of globoid cell leukodystrophy. Faseb J. 2005 Sep; 19(11):1549–1551. [PubMed: 15987783]

20. Matsushima GK, Taniike M, Glimcher LH, Grusby MJ, Frelinger JA, Suzuki K, et al. Absence of MHC class II molecules reduces CNS demyelination, microglial/macrophage infiltration, and twitching in murine globoid cell leukodystrophy. Cell. 1994 Aug 26; 78(4):645–656. [PubMed: 8069913]

21. Kyzar E, Gaikwad S, Roth A, Green J, Pham M, Stewart A, et al. Towards highthroughput phenotyping of complex patterned behaviors in rodents: focus on mouse selfgrooming and its sequencing. Behav Brain Res. 2011 Dec 1; 225(2):426–431. [PubMed: 21840343]

22. Moscardo E, Rostello C. An integrated system for video and telemetric electroencephalographic recording to measure behavioural and physiological parameters. J Pharmacol Toxicol Methods. 2010 Jul-Aug;62(1):64–71. [PubMed: 20435150]

23. Noldus LP, Spink AJ, Tegelenbosch RA. EthoVision: a versatile video tracking system for automation of behavioral experiments. Behav Res Methods Instrum Comput. 2001 Aug; 33(3): 398–414. [PubMed: 11591072]

24. Spink AJ, Tegelenbosch RA, Buma MO, Noldus LP. The EthoVision video tracking system--a tool for behavioral phenotyping of transgenic mice. Physiol Behav. 2001 Aug; 73(5):731–744. [PubMed: 11566207]

25. Terrell KA, Rasmussen TA, Trygg C, Bunnell BA, Buck WR. Molecular beacon genotyping for globoid cell leukodystrophy from hair roots in the twitcher mouse and rhesus macaque. J Neurosci Methods. 2007 Jun 15; 163(1):60–66. [PubMed: 17412425]

26. Schindelin J, Arganda-Carreras I, Frise E, Kaynig V, Longair M, Pietzsch T, et al. Fiji: an open-source platform for biological-image analysis. Nat Methods. 2012; 9(7):676–682. [PubMed: 22743772]

27. Kalueff AV, Fox MA, Gallagher PS, Murphy DL. Hypolocomotion, anxiety and serotonin syndrome-like behavior contribute to the complex phenotype of serotonin transporter knockout mice. Genes Brain Behav. 2007 Jun; 6(4):389–400. [PubMed: 16939636]

28. Christomanou H, Jaffe S, Martinius J, Cap C, Betke K. Biochemical, genetic, psychometric, and neuropsychological studies in heterozygotes of a family with globoid cell leucodystrophy (Krabbe's disease). Hum Genet. 1981; 58(2):179–183. [PubMed: 7287002]

29. Farrimond JA, Hill AJ, Jones NA, Stephens GJ, Whalley BJ, Williams CM. A costeffective high-throughput digital system for observation and acquisition of animal behavioral data. Behav Res Methods. 2009 May; 41(2):446–451. [PubMed: 19363185]
30. Meyerrose TE, Roberts M, Ohlemiller KK, Vogler CA, Wirthlin L, Nolta JA, et al. Lentiviral-transduced human mesenchymal stem cells persistently express therapeutic levels of enzyme in a xenotransplantation model of human disease. Stem Cells. 2008 Jul; 26(7):1713–1722. [PubMed: 18436861]
31. Lanz TV, Opitz CA, Ho PP, Agrawal A, Lutz C, Weller M, et al. Mouse mesenchymal stem cells suppress antigen-specific TH cell immunity independent of indoleamine 2,3- dioxygenase 1 (IDO1). Stem Cells Dev. 2010 May; 19(5):657–668. [PubMed: 19886804]
32. Crawley JN. Behavioral phenotyping of transgenic and knockout mice: experimental design and evaluation of general health, sensory functions, motor abilities, and specific behavioral tests. Brain Res. 1999 Jul 17; 835(1):18–26. [PubMed: 10448192]
33. Miller BH, Schultz LE, Gulati A, Su AI, Pletcher MT. Phenotypic characterization of a genetically diverse panel of mice for behavioral despair and anxiety. PLoS One. 2010; 5(12):e14458. [PubMed: 21206921]
34. Kalueff AV, Aldridge JW, LaPorte JL, Murphy DL, Tuohimaa P. Analyzing grooming microstructure in neurobehavioral experiments. Nat Protoc. 2007; 2(10):2538–2544. [PubMed: 17947996]
35. Sachs BD. The development of grooming and its expression in adult animals. Ann N Y Acad Sci. 1988; 525:1–17. [PubMed: 3291663]
36. Kalueff AV, Tuohimaa P. Contrasting grooming phenotypes in C57Bl/6 and 129S1/SvImJ mice. Brain Res. 2004 Nov 26; 1028(1):75–82. [PubMed: 15518644]
37. Kalueff AV, Tuohimaa P. Contrasting grooming phenotypes in three mouse strains markedly different in anxiety and activity (129S1, BALB/c and NMRI). Behav Brain Res. 2005 May 7; 160(1):1–10. [PubMed: 15836895]
38. Coscia EM, Fentress JC. Neurological dysfunction expressed in the grooming behavior of developing weaver mutant mice. Behav Genet. 1993 Nov; 23(6):533–541. [PubMed: 8129695]
39. Uccelli A, Benvenuto F, Laroni A, Giunti D. Neuroprotective features of mesenchymal stem cells. Best Pract Res Clin Haematol. 2011 Mar; 24(1):59–64. [PubMed: 21396593]
40. Chen X, Armstrong MA, Li G. Mesenchymal stem cells in immunoregulation. Immunol Cell Biol. 2006 Oct; 84(5):413–421. [PubMed: 16869941]
41. Hardy SA, Maltman DJ, Przyborski SA. Mesenchymal stem cells as mediators of neural differentiation. Curr Stem Cell Res Ther. 2008 Jan; 3(1):43–52. [PubMed: 18220922]
42. Croitoru-Lamoury J, Williams KR, Lamoury FM, Veas LA, Ajami B, Taylor RM, et al. Neural transplantation of human MSC and NT2 cells in the twitcher mouse model. Cytotherapy. 2006; 8(5):445–458. [PubMed: 17050249]
43. Gimble JM, Katz AJ, Bunnell BA. Adipose-derived stem cells for regenerative medicine. Circ Res. 2007 May 11; 100(9):1249–1260. [PubMed: 17495232]
44. Koc ON, Peters C, Aubourg P, Raghavan S, Dyhouse S, DeGasperi R, et al. Bone marrow-derived mesenchymal stem cells remain host-derived despite successful hematopoietic engraftment after allogeneic transplantation in patients with lysosomal and peroxisomal storage diseases. Exp Hematol. 1999 Nov; 27(11):1675–1681. [PubMed: 10560915]
45. Duchen LW, Eicher EM, Jacobs JM, Scaravilli F, Teixeira F. Hereditary leucodystrophy in the mouse: the new mutant twitcher. Brain. 1980 Sep; 103(3):695–710. [PubMed: 7417782]
46. Smith B, Galbiati F, Cantuti-Castelvetri L, Givogri MI, Lopez-Rosas A, Bongarzone ER. Peripheral neuropathy in the Twitcher mouse involves the activation of axonal caspase 3. ASN Neuro. 2011 Sep 19.
47. Scaravilli F, Suzuki K. Enzyme replacement in grafted nerve of twitcher mouse. Nature. 1983 Oct 20–26; 305(5936):713–715. 1983. [PubMed: 6633639]
48. Duffner PK, Barczykowski A, Jalal K, Yan L, Kay DM, Carter RL. Early infantile Krabbe disease: results of the World-Wide Krabbe Registry. Pediatr Neurol. 2011 Sep; 45(3):141–148. [PubMed: 21824559]

49. Duffner PK, Barczykowski A, Kay DM, Jalal K, Yan L, Abdelhalim A, et al. Later onset phenotypes of Krabbe disease: results of the world-wide registry. Pediatr Neurol. 2012 May; 46(5):298–306. [PubMed: 22520351]
50. Barone R, Brðhl K, Stoeter P, Fiumara A, Pavone L, Beck M. Clinical and neuroradiological findings in classic infantile and late-onset globoid-cell leukodystrophy (Krabbe disease). Am J Med Genet. 1996 May; 63(1):209–217. [PubMed: 8723112]
51. Zafeiriou DI, Anastasiou AL, Michelakaki EM, Augoustidou-Savvopoulou PA, Katzos GS, Kontopoulos EE. Early infantile Krabbe disease: deceptively normal magnetic resonance imaging and serial neurophysiological studies. Brain Dev. 1997 Nov; 19(7):488–491. [PubMed: 9408597]
52. Sasaki M, Sakuragawa N, Takashima S, Hanaoka S, Arima M. MRI and CT findings in Krabbe disease. Pediatr Neurol. 1991 Jul-Aug;7(4):283–288. 1991. [PubMed: 1930420]
53. Puckett RL, Orsini JJ, Pastores GM, Wang RY, Chang R, Saavedra-Matiz CA, et al. Krabbe disease: clinical, biochemical and molecular information on six new patients and successful retrospective diagnosis using stored newborn screening cards. Mol Genet Metab. 2012 Jan; 105(1): 126–131. [PubMed: 22115770]
54. Hagberg B, Kollberg H, Sourander P, Akesson HO. Infantile globoid cell leucodystrophy (Krabbe's disease). A clinical and genetic study of 32 Swedish cases 1953--1967. Neuropadiatrie. 1969 Jun-Jul;1(1):74–88. 1969. [PubMed: 5409293]
55. Brownsworth RD, Bodensteiner JB, Schaefer GB, Barnes P. Computed tomography and magnetic resonance imaging in late-onset globoid cell leukodystrophy (Krabbe disease). Pediatr Neurol. 1985 Jul-Aug;(4):242–244. 1985. [PubMed: 3880410]

Highlights

- Novel biomarkers of the twitcher mouse were detected using an automated system
- Intraperitoneal injections of stem cells were administered to twitcher mice
- Twitcher mice receiving cell therapy had improved locomotion and motor function
- Automated analysis of mouse behavior is effective as therapeutic screening for GLD

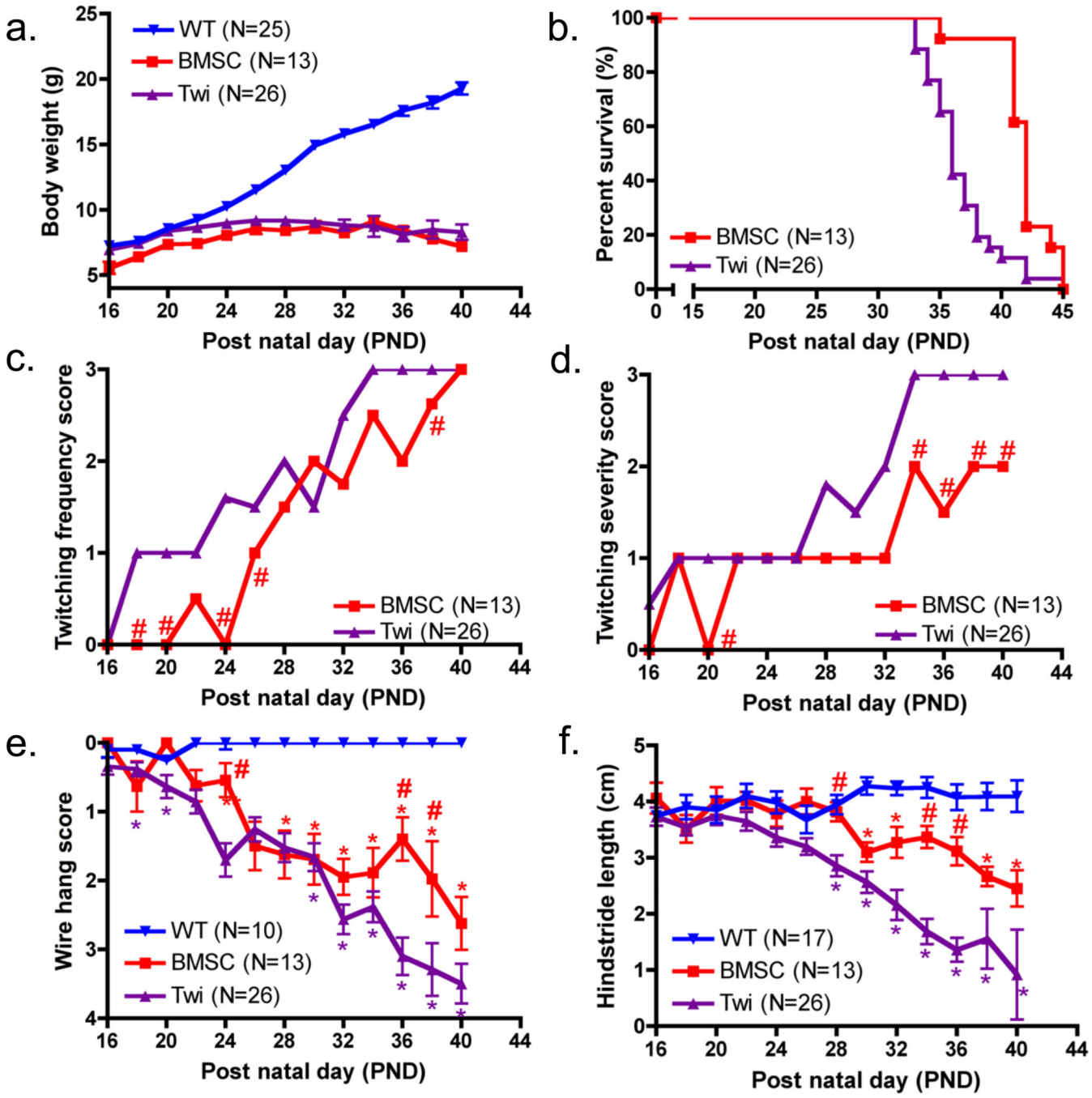

Figure 1. Weight, lifespan and motor function after IP transplantation of BMSCs

(a) Body weight was measured three times a week for untreated WT, BMSC-treated twitcher, and untreated twitcher mice starting at PND 16. (b) All twitcher mice (BMSC and Twi) were monitored daily and euthanized at 20% of the maximum body weight or when they became moribund. A Kaplan-Meier survival curve of the untreated and BMSC treated twitcher groups is shown. (c and d) Twitching frequency and severity were assessed three times a week for all twitcher mice using the conventional twitching clinical scoring systems. Medians, and not means, are plotted, and significant differences between the two treatment groups are indicated by # if $P<0.0038$, (e) Hind leg strength was assessed for untreated WT, BMSC-treated twitcher, and untreated twitcher mice three times a week using the wire hang

test. Significant differences between the Twi mice and BMSC or WT groups are indicated by # or *, respectively, if P<0.0012. (f) Hind stride was measured for untreated WT, BMSC-treated twitcher, and untreated twitcher mice three times a week for assessment of gait. Significant differences between the Twi mice and BMSC or WT groups are denoted by # or *, respectively, if P<0.0014.

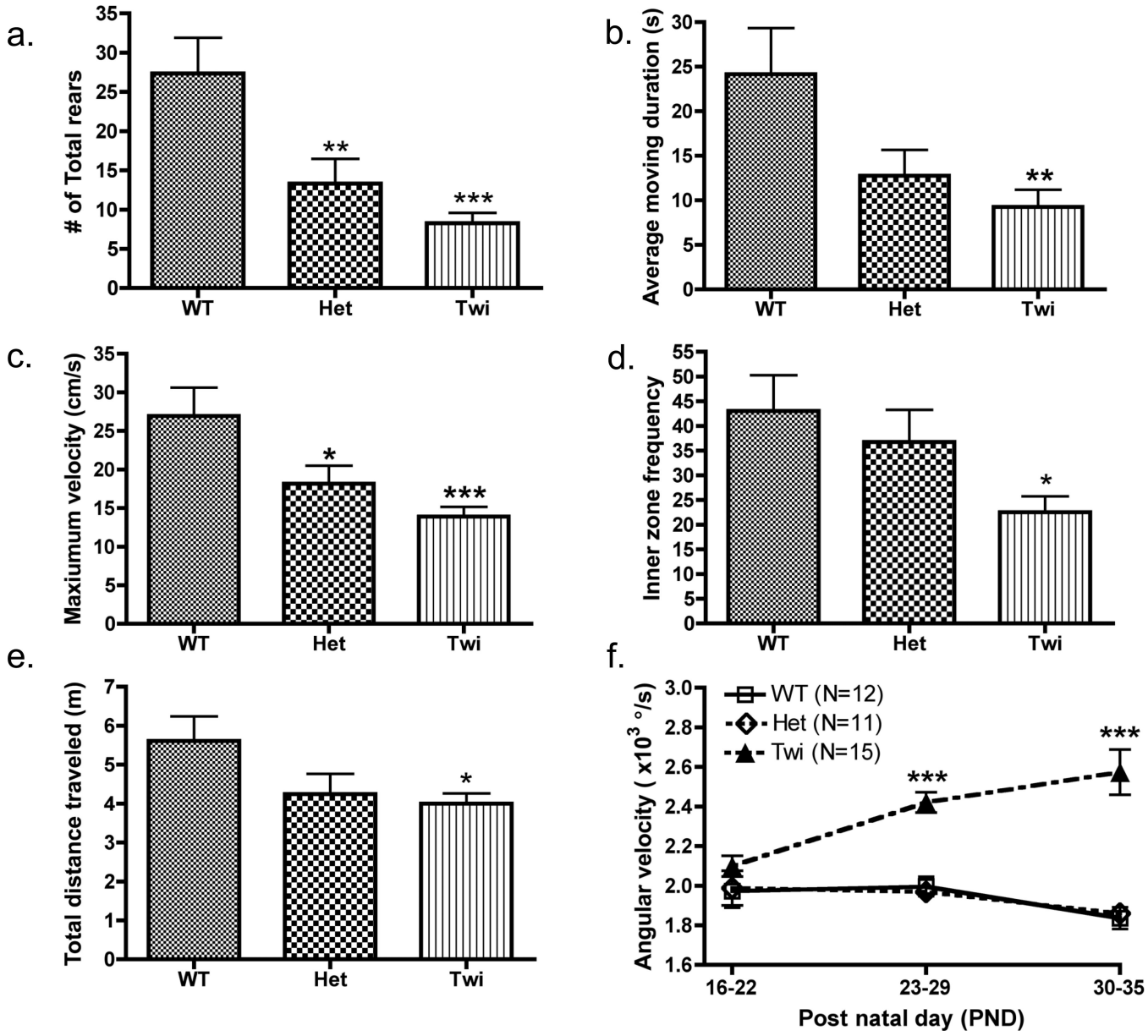

Figure 2. Assessment of behavioral and physiological differences in mice of different genotypes

(a) The number of protected rears was manually observed for all untreated GLD mouse groups (WT (N=9), Het (N=13), and Twi (N=18)). Computer-automated values were generated using EthoVision XT7 software for (b) average moving duration (c) maximum velocity, (d) inner zone frequency, and (e) total distance traveled; all mice (WT (N=12), Het (N=13), and Twi (N=19)) were observed only once during the period of PND16–22. (f) Angular velocity was monitored for a select few mice from each group (WT (N=12), Het (N=11), and Twi (N=15)) over three consecutive weeks (PND 16–22, 23–29, and 30–35). Comparisons between the three genotype groups were made by Bonferroni's *posthoc* testing following one-way ANOVA (a–e) or two-way ANOVA with repeated measures (f). Significant differences are denoted by *P<0.05, **P<0.01 and ***P<0.001 vs. WT mice.

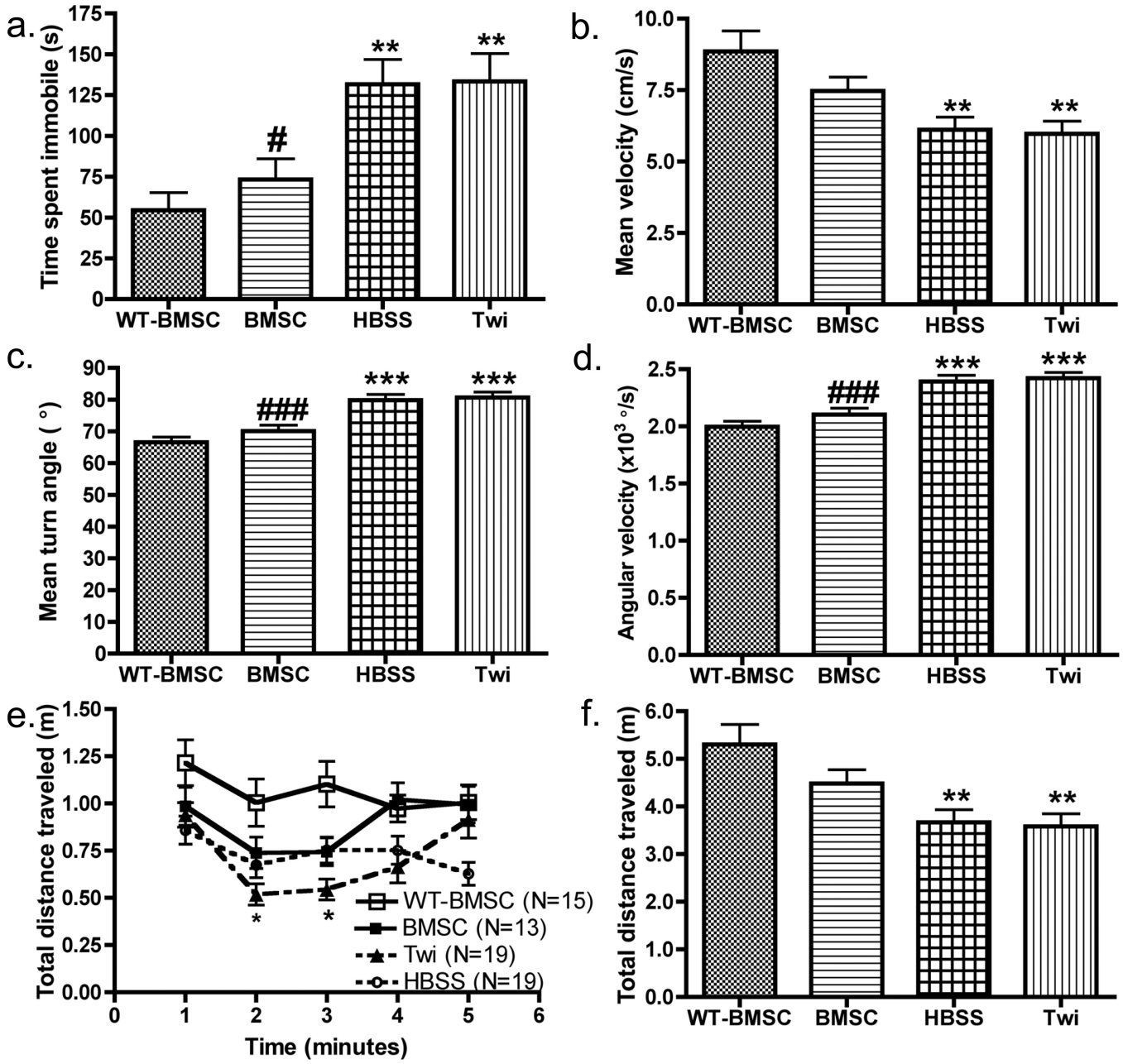

Figure 3. Assessment of physiological effects after IP treatment using automated video-tracking

Comparative analysis of (a) average time spent immobile, (b) average velocity, (c) mean turn angle, (d) angular velocity, (e) distance traveled for each minute of the recording period, and (f) total distance traveled for four mouse groups (BMSC-treated WT (WT-BMSC, N=15), BMSC-treated twitcher (BMSC, N=13), HBSS-injected twitcher (HBSS, N=19), and untreated twitcher (Twi, N=19) mice). All mice were observed once during the period of PND23–29, and comparisons between the four mouse groups were made by Bonferroni's *post-hoc* testing following one-way ANOVA (a–d, f) or two-way ANOVA with repeated measures (e). Significant differences are denoted by *P<0.05, **P<0.01 and ***P<0.001 vs. WT-BMSC mice.

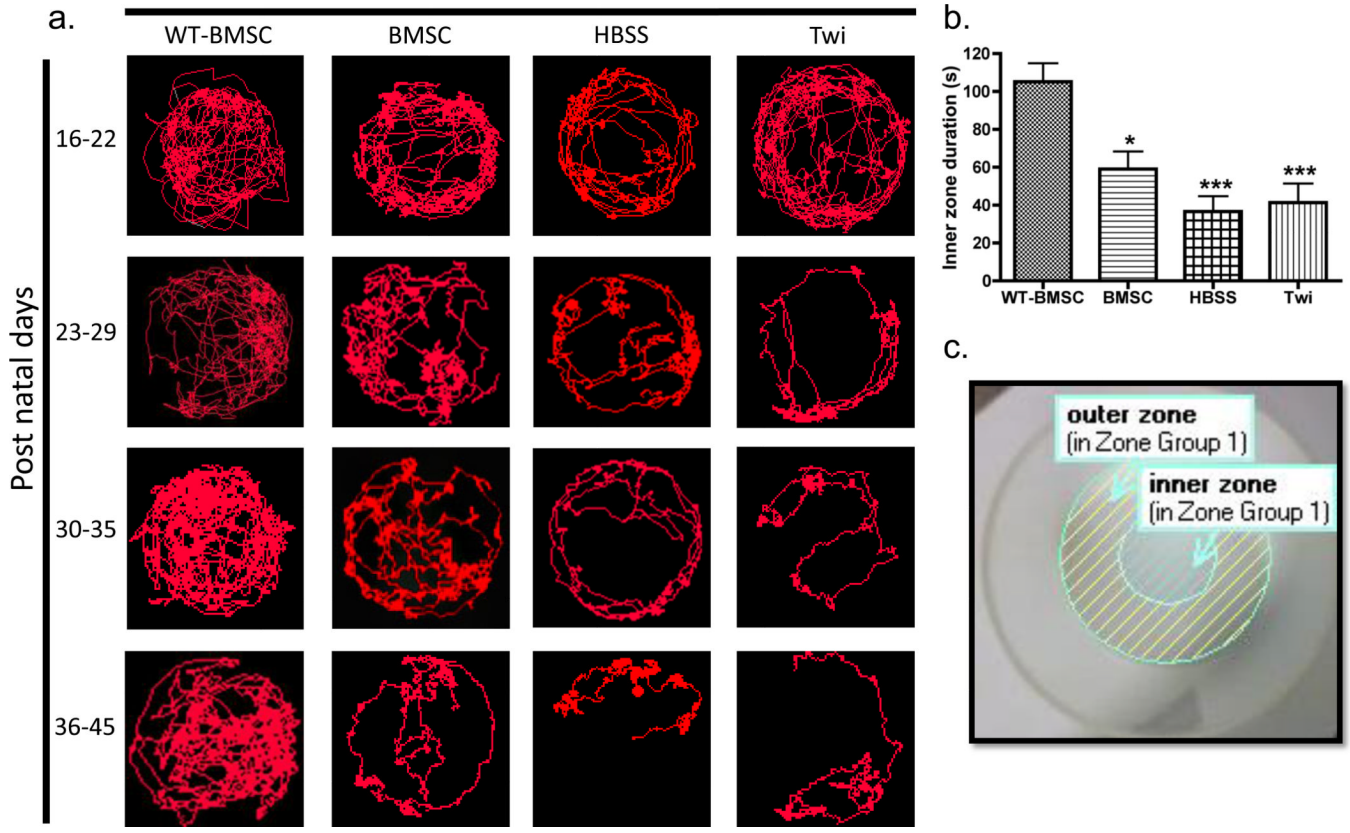

Figure 4. Monitoring disease progression by comparison of track visualizations

(a) Representative images of sixteen mouse tracks are shown. These tracks were chosen as previously described for each of the four mouse groups over four consecutive weeks, PND16–22, 23–29, 30–35, and 36–45. For any given time period, a mouse was recorded once for 5 min, and Ethovision XT7 was used to generate the visualization of the mouse tracks. The HBSS-injected (HBSS) and untreated (Twi) twitcher tracks show a marked decrease in track density, especially in the inner zone of the arena, seen as early as PND 23–29. (b) The duration of time spent in the inner zone over 5 min (i.e., inner zone duration) was compared for BMSC-treated twitcher (BMSC, N=13), HBSS-injected mice (HBSS, N=19), non-injected twitcher (Twi, N=19), and BMSC-treated WT (WT-BMSC, N=15) mice. Comparisons between mouse groups were made using one-way ANOVA and Bonferroni's *post-hoc* testing, where *P<0.05; **P<0.01; ***P<0.001 vs. WTBMSC. (c) A representative arena setting using EthoVision XT7 is shown with designated inner and outer zones for assessing thigmotaxis.

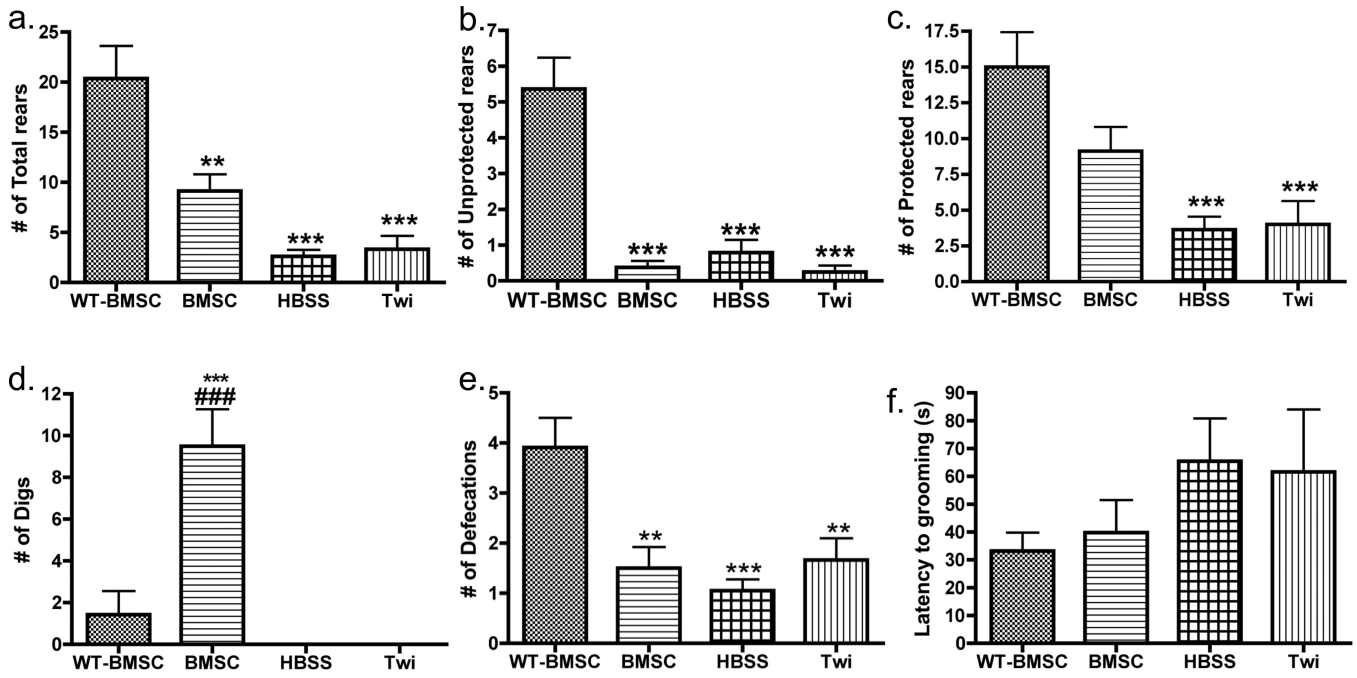

Figure 5. Behavioral differences between genotype and treatment groups detected by manual observation

Comparative analysis of (a) the number of total rearing episodes, (b) the number of protected rearing episodes, (c) the number of unprotected rearing episodes, (d) the number of digs manually observed, (e) the number of defecations, and (f) the latency to grooming activity for four mouse groups (BMSC-treated twitcher (BMSC, N=13), HBSS-injected twitcher (HBSS, N=19), untreated twitcher (Twi, N=12) and BMSC-treated WT (WT-BMSC, N=11) mice). All mice were observed only once during the period of PND23–29, and comparisons between genotype were made using one-way ANOVA and Bonferroni's *post-hoc* testing. Significant differences are denoted by *P<0.05; **P<0.01; ***P<0.001 vs. WT-BMSC mice and ###p<0.001 vs. Twi.

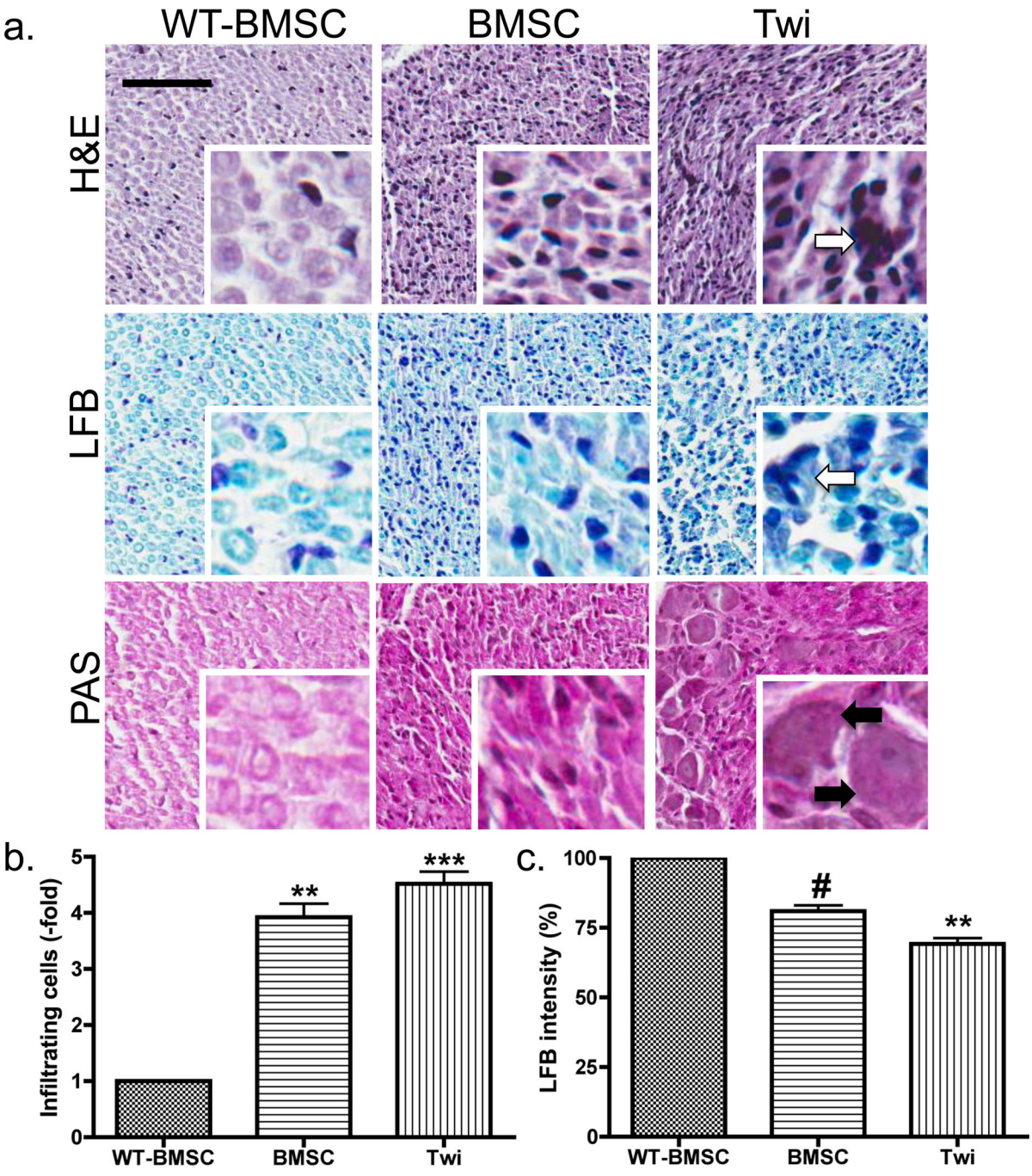

Figure 6. Histological staining of sciatic nerves

(a) Sciatic nerves from BMSC-treated WT, BMSC-treated twitcher, and untreated twitcher mice were obtained after euthanasia at PND37 and processed for histological staining using Hematoxylin and Eosin (HE), Luxol Fast Blue (LFB), and Periodic Acid-Schiff (PAS) stains. The scale bar represents 50 microns for all larger images (10X), and each smaller image (40X) is a fourfold magnification of the larger image. Comparisons of the HE, LFB, and PAS images of the twitcher mouse sciatic nerves show a decrease in the number of apoptotic cells (white arrows) and infiltrating immune cells (black arrows) in the PNS after IP administration of BMSCs. (b) The number of infiltrating immune cells in the HE stains of the WT-BMSC (N=5), BMSC (N=4), and Twi (N=8) groups were calculated, compared to

the total pixels for each scanned image, and normalized to the WT-BMSC group. (c) The staining intensity in the LFB stains of the WT (n=3), BMSC (n=4), and Twi (n=7) groups were calculated, compared to the total pixels for each scanned image, and normalized to the WT-BMSC group. Following one-way ANOVA, comparisons were made using Bonferroni's *post-hoc* testing. Significant differences are denoted by *P<0.05; **P<0.01; ***P<0.001 vs. WT-BMSC and #P<0.05 vs. Twi mice.

Table 1

GLD mouse genotype-related differences in physical characteristics, computer-automated spatial and arena parameters, and manually observed behaviorduring PND 16–22

Variables calculated from tracks using EthoVision XT7 and manual behavior observations are provided for untreated WT, Het, and twitcher mice. The ratio of males (M) to females (F) is provided for each group as (M/F). One-way ANOVA was performed with the three mouse groups, and comparisons between the WT and Twi groups were made using Bonferroni's *post-hoc* tests.

	WT ($Galc^{+/+}$)	Het ($Galc^{twi/+}$)	Twi ($Galc^{twi/twi}$)	
	Mean±SEM	**Mean±SEM**	**Mean±SEM**	**WT v. Twi**
Characteristics				
Average Age (Post natal day)	20.44±0.40	21.46±0.40	18.28±0.6	
Average Body weight (g), PND 20	8.56±0.30	8.72±0.24	7.34±0.12	
Spatial Parameters				
Number of animals (M/F)	12 (6/6)	13 (5/8)	19(10/9)	
Total distance traveled (m)	5.61±0.63	4.24±0.52	4.00±0.26	*
Average velocity (cm/s)	1.88±0.21	1.49±0.17	1.40±0.10	
Maximum velocity (cm/s)	26.94±3.66	18.17±2.33	13.90±1.26	***
Angular velocity (°/s)	1973±84.07	1988±87.39	2098±52.36	
Mean turn angle (°)	65.76±2.80	66.28±2.91	69.95±1.75	
Total meandering ($\times 10^8$ °/m)	2.67±0.44	4.28±0.92	3.82±0.43	
Moving duration (s)	24.16±5.17	12.76±2.92	9.26±1.94	**
Moving frequency (#)	1.72±0.17	1.54±0.11	1.22±0.13	*
Time spent immobile (s)	76.35±19.96	96.01±15.78	104.30±15.78	
Inner zone frequency (#)	43.00±7.234	36.73±6.527	22.53±3.20	*
Inner zone duration (s)	42.89±8.95	59.52±14.52	34.23±7.03	
Behavioral Endpoints				
Number of animals (M/F)	9 (4/5)	13 (5/8)	18(9/9)	
Latency to groom (s)	19.22±3.23	23.27±3.21	37.76±6.74	
Paw lick duration (s)	15.78±2.52	13.08±1.08	20.94±3.15	
Body/leg wash duration (s)	15.38±4.33	15.92±4.51	13.28±3.60	
Number of unprotected rears	9.89±2.26	3.54±1.39	1.56±0.45	**
Number of protected rears	17.44±3.31	9.77±1.87	6.72±0.99	***
Number of total rears	27.33±4.56	13.31±3.15	8.28±1.30	***
Number of defecations	2.22+0.55	1.92+0.49	1.83+0.44	

* P<0.05;

** P<0.01;

*** P<0.001 vs. WT.

Table 2

GLD mouse genotype and treatment-related differences in physical characteristics, computer-automated spatial and arena parameters, and manually observed behavior during PND23–29

Variables calculated from tracks using EthoVision XT7 and manual behavior observations are provided for BMSC-treated WT (WT-BMSC), BMSC-treated twitcher (BMSC), HBSS-injected twitcher (HBSS), and untreated twitcher (Twi) mice. The ratio of males (M) to females (F) is provided for each group as (M/F). Oneway ANOVA was performed for the four mouse groups, and comparisons between the groups were made using Bonferroni's *post-hoc* testing.

	WT-BMSC ($Galc^{+/+}$)	BMSC ($Galc^{twi/twi}$)		HBSS ($Galc^{twi/twi}$)		Twi (($Galc^{twi/twi}$))	
	Mean±SEM	Mean±SEM	BMSC v. WT (*) BMSCv. HBSS(†) BMSC v. Twi (#)	Mean±SEM	HBSS v. WT (*)	Mean±SEM	Twi v. WT (*)
Characteristics							
Average age (PND)	25.20±0.35	25.60±0.50		26.52±0.14		26.40±0.53	
Average weight (g), PND 25	11.78±0.31	8.46±0.32	***	9.31±0.17	***	9.10±0.31	***
Spatial Parameters							
Number of animals (M/F)	15(8/7)	13 (6/7)		19(9/10)		19(10/9)	
Total distance traveled (m)	5.30±0.42	4.48±0.29		3.67±0.27	**	3.58±0.27	**
Average velocity (cm/s)	8.86±0.72	7.47±0.48		6.11±0.44	**	5.97±0.45	**
Maximum velocity (cm/s)	25.65±3.32	18.43±1.80		15.05±2.57	*	14.82±2.55	*
Angular velocity (°/s)	1996±49.54	2103±55.40	###, ††	2392±54.19	***	2421±51.31	***
Mean turn angle (°)	66.54±1.65	70.10±1.85	###, ††	79.82±1.81	***	80.70±1.71	***
Average moving duration (s)	17.04±3.40	10.09±1.79		5.33±1.03	***	6.33±1.36	**
Moving frequency	1.50±0.14	1.08±0.08		0.83±0.12	***	0.83±0.10	***
Average time immobile (s)	54.47±10.77	73.34±12.66	#	131.6±15.18	**	133.30±17.03	**
Inner zone frequency	54.73±6.03	38.54±5.47	††	12.47±2.04	***	23.84±6.08	***
Inner zone duration (s)	105.10±9.83	54.54±9.67		46.71±12.66	**	56.01±13.97	*
Behavioral Endpoints							
Number of animals (M/F)	11 (4/7)	13 (6/7)		19(9/10)		12(7/5)	
Latency to groom (s)	33.20±6.62	39.75±11.71		61.60±22.45		65.47±15.34	
Paw lick duration (s)	14.27±1.53	22.13±4.96		21.05±4.13		19.50±3.96	
Body/leg wash duration (s)	7.46±1.82	5.50±1.76		5.32±2.24		5.00±2.43	
Number of unprotected rears	5.36±0.88	0.38±0.18	***	0.79±0.36	***	0.25±0.18	***

	WT-BMSC (Galc$^{+/+}$)	BMSC (Galc$^{twi/twi}$)		HBSS (Galc$^{twi/twi}$)		Twi ((Galc$^{twi/twi}$))	
	Mean±SEM	**Mean±SEM**	**BMSC v. WT (*) BMSCv. HBSS(†) BMSC v. Twi (#)**	**Mean±SEM**	**HBSS v. WT (*)**	**Mean±SEM**	**Twi v. WT (*)**
Number of protected rears	15.00±2.44	9.13±1.68		3.63±0.92	***	4.00±1.64	***
Number of total rears	20.36±3.25	9.50±1.68	**	2.61±0.66	***	3.33±1.32	***
Number of defecations	3.91±0.59	1.50±0.42	**	1.05±0.22	***	1.67±0.43	**
Number of digs	1.43±1.13	9.50±1.76	***, ###, †††	0.00		0.00	

*P<0.05;

**P<0.01;

***P<0.001 vs. WT-BMSC.

#P<0.05;

##P<0.01;

###P<0.001 vs. Twi.

†P<0.05;

††P<0.01;

†††P<0.001 vs. HBSS.